

Natural variation identifies a *Pxy* gene controlling vascular organisation and formation of nodules and lateral roots in *Lotus japonicus*

Yasuyuki Kawaharada^{1,2} , Niels Sandal² , Vikas Gupta², Haojie Jin² , Maya Kawaharada¹, Makoto Taniuchi¹, Hafijur Ruman³, Marcin Nadzieja², Kasper R. Andersen² , Korbinian Schneeberger⁴ , Jens Stougaard²  and Stig U. Andersen² 

¹Department of Plant BioSciences, Faculty of Agriculture, Iwate University, 3-18-8 Ueda, Morioka, Iwate, Japan; ²Department of Molecular Biology and Genetics, Aarhus University, Aarhus C 8000, Denmark; ³United Graduate School of Agricultural Sciences, Iwate University, 3-18-8 Ueda, Morioka, Iwate, Japan; ⁴Department for Plant Developmental Biology, Max Planck Institute for Plant Breeding Research, Cologne 50829, Germany

Authors for correspondence:

Yasuyuki Kawaharada

Email: yasuyuki@iwate-u.ac.jp

Stig U. Andersen

Email: sua@mbg.au.dk

Received: 7 October 2020

Accepted: 1 March 2021

New Phytologist (2021) 230: 2459–2473

doi: 10.1111/nph.17356

Key words: legume, *Lotus japonicus*, natural variation, QTL, *Rhizobium*, symbiosis.

Summary

- Forward and reverse genetics using the model legumes *Lotus japonicus* and *Medicago truncatula* have been instrumental in identifying the essential genes governing legume–rhizobia symbiosis. However, little is known about the effects of intraspecific variation on symbiotic signalling.
- Here, we use quantitative trait locus sequencing (QTL-seq) to investigate the genetic basis of the differentiated phenotypic responses shown by the *Lotus* accessions Gifu and MG20 to inoculation with the *Mesorhizobium loti* *exoU* mutant that produces truncated exopolysaccharides.
- Through genetic complementation, we identify the *Pxy* gene as a component of this differential *exoU* response. *Lotus Pxy* encodes a leucine-rich repeat receptor-like kinase similar to *Arabidopsis thaliana* PXY, which regulates stem vascular development. We show that *Lotus pxy* insertion mutants display defects in root and stem vascular organisation, as well as lateral root and nodule formation.
- Our work links *Pxy* to *de novo* organogenesis in the root, highlights the genetic overlap between regulation of lateral root and nodule formation, and demonstrates that natural variation in *Pxy* affects nodulation signalling.

Introduction

The symbiotic interaction between legumes and rhizobia results in the development of new organs called root nodules. These symbiotic organs are established by two tightly synchronised processes, bacterial infection and nodule organogenesis. Rhizobia sense specific flavonoids from host legume plants and, in response, rhizobia synthesise and secrete lipochito-oligosaccharides (Nod factors) that serve as specific symbiotic signal molecules (D’Haeze & Holsters, 2002) and establish a two-way recognition system. In the model legume *Lotus japonicus* (*Lotus*), NFR1, NFR5 and NFR6 lysin motif (LysM) receptors perceive rhizobial Nod factors (Madsen *et al.*, 2003; Radutoiu *et al.*, 2003; Broghammer *et al.*, 2012; Murakami *et al.*, 2018). In subsequent steps NFR5 interacts with the SYMRK LRR receptor and a cytoplasmic kinase NiCK4 that accelerates downstream signalling (Antolín-Llovera *et al.*, 2014; Wong *et al.*, 2019). A role for bacterial exopolysaccharides in recognition and signalling has been found in both *Lotus* and *Medicago truncatula* (*Medicago*)

(Maillet *et al.*, 2020). In *Lotus*, the *Epr3* gene is transcriptionally upregulated by NFR1/NFR5-mediated Nod factor signalling, and exopolysaccharide perception constitutes a second compatibility check of the bacterial symbionts. Wild-type octasaccharide or the truncated pentasaccharide secreted by *exoU* mutants of *Mesorhizobium loti* and perceived by the EPR3 receptor has a positive, respectively negative, effect on infection thread formation (Kawaharada *et al.*, 2015, 2017b). Further downstream in the symbiosis pathway operating in *Lotus* and/or *Medicago*, nucleoporins (NUP85, NUP133 and NENA), cation channels (CASTOR and POLLUX) and calcium channels (CNGC) are involved in releasing the perinuclear calcium spiking (Ané *et al.*, 2004; Imaizumi-Anraku *et al.*, 2005; Kanamori *et al.*, 2006; Saito *et al.*, 2007; Charpentier *et al.*, 2008, 2016; Groth *et al.*, 2010; Chiasson *et al.*, 2017) that is recorded by calcium calmodulin-dependent protein kinases (CCaMK) (Lévy *et al.*, 2004; Mitra *et al.*, 2004; Gleason *et al.*, 2006; Singh & Parniske, 2012). A set of transcription factors (CYCLOPS, NSP1, NSP2, ERN1, NIN and NF-Ys) is then required for organogenesis and/or

infection thread formation (Schäuser *et al.*, 1999; Heckmann *et al.*, 2006; Middleton *et al.*, 2007; Hirsch *et al.*, 2009; Cerri *et al.*, 2017; Kawaharada *et al.*, 2017a; Yano *et al.*, 2017). Infection thread formation involves a pectate lyase, *NPL*, actin rearrangement by NAP1, PIR1, SCARN, ARPC1 and DREPP, an E3 ubiquitin ligase, an atypical receptor kinase *RINRK*, a subunit of mediator complex *LAN*, and novel functions encoded by *Rpg*, *Vapyrin* and *CBS* (Arrighi *et al.*, 2008; Yano *et al.*, 2009; Yokota *et al.*, 2009; Murray *et al.*, 2011; Hossain *et al.*, 2012; Xie *et al.*, 2012; Qiu *et al.*, 2015; Sinharoy *et al.*, 2016; Li *et al.*, 2019; Suzaki *et al.*, 2019; Su *et al.*, 2020). Localised changes in plant hormone homeostasis (cytokinin, auxin and jasmonic acid) regulate the initiation of infection thread formation and cell divisions leading to nodule organogenesis (Suzuki *et al.*, 2011; Reid *et al.*, 2017; Nadzieja *et al.*, 2018, 2019). By contrast, ethylene and abscisic acid suppress nodule formation (Nukui *et al.*, 2000; Tominaga *et al.*, 2009; Reid *et al.*, 2018).

Distinct mutant phenotypes and monogenic inheritance is the foundation for the characterisation of these central pathways that are highly conserved across model legumes highlighting the importance of the core components of the symbiosis pathway.⁴⁸ Interspecific and intraspecific differences reflecting natural variation have, however, also been found. One such example is the influence of rhizobial exopolysaccharides on root nodule development, primarily infection thread formation. Classical genetic and biochemical studies using the Lotus Gifu accession have shown that the EPR3 receptor perceives and recognises EPS produced by *M. loti* and controls infection thread formation (Kawaharada *et al.*, 2015, 2017b).

Interestingly, variability in exopolysaccharide responses towards truncated exopolysaccharide synthesised by the *M. loti* *exoU* mutant was found among 65 Lotus natural accessions (Kelly *et al.*, 2013). Like Gifu, 15 Lotus accessions formed only white, uninfected nodule primordia. A less stringent response was observed for 45 other accessions where up to 50% of the plants developed at least one pink infected nodule, and an intermediate response was found in eight accessions, including MG20, that developed pink nodules on 50–75% of the plants. Such quantitative phenotypic differences suggest that there are complex multigene traits involved in diversification of nodulation signalling. These traits could be controlled by genetic components different to those discovered through forward genetic screens, but could potentially be identified by means of quantitative genetics approaches.

Here, we use quantitative trait locus sequencing (QTL-seq) to identify *Pxy* as a causal component of the differential *exoU* response and show that *Pxy* is required for normal vascular organisation and lateral root and nodule formation in Lotus.

Materials and Methods

Plant materials and growth conditions

Plant seeds for analysis of the nodulation phenotype with *M. loti* strains were germinated and grown on quarter-strength B&D medium or modified Long Ashton medium (Supporting

information Table S1) including 1.4% agar covered with filter paper in Petri dishes. The plant roots were shielded from light using a metal comb fitting the Petri dish and inserting the lower half of the plates into a rack to keep the root dark. Alternatively, plants were grown in magenta plastic containers in a 4 : 1, LECA : Vermiculite mixture supplemented with 60 ml quarter-strength B&D per container for complementation analysis. These plants were inoculated with 500–1000 μ l *M. loti* R7A wild-type or *exoU* (Kelly *et al.*, 2013) culture at OD₆₀₀ = 0.01–0.04 per plate and magenta box. Plants were grown at 21°C under 16 h : 8 h, light : dark conditions. Heterozygous *pxy* *LORE1* mutant plants were grown for harvesting seeds. Homozygous mutants were selected using PCR for each experiment (Table S2).

Gene and CDS cloning

For the overexpression constructs, the *Xdh2* and *Pxy* genes were amplified from Lotus Gifu and MG20 genomic DNA using PCR and primers (*Xdh2*; 5'-TCCTAGCTATGAGTTCTCTCA-3' and 5'-CTAGCTAGCATTCCAAGGGA-3', *Pxy*; 5'-ACCCCAAACCATGAACCT-3'; and 5'-CATATAAACAGATTAAATCAGC-3') containing attB sites. The *Smc6* CDS was amplified from Lotus Gifu and MG20 cDNA from root and nodule tissues, which were produced using the 5'-SMART RACE cDNA amplification kit (Clontech), using PCR using primers (*Smc6*; 5'-CCGGCGTTTGCAGAATGAAGCGGAGA-3' and 5'-GAGATTGAACATGATGAAACGCAG-3') containing attB sites. The PCR amplification products were recombined into pDONR207 (Invitrogen) using Gateway BP reactions (Invitrogen) to create entry clone vectors. The entry clone vectors were recombined using Gateway LR reactions (Invitrogen) with the destination vector pIV10::Ubiquitin_promoter:GW, to create the constructs: pIV10::Ubiquitin_promoter:Gifu_*Xdh2*, pIV10::Ubiquitin_promoter:MG20_*Xdh2*, pIV10::Ubiquitin_promoter:Gifu_*Pxy*, pIV10::Ubiquitin_promoter:MG20_*Pxy*, pIV10::Ubiquitin_promoter:Gifu_*Smc6* and pIV10::Ubiquitin_promoter:MG20_*Smc6*. For complementation analysis, *Agrobacterium rhizogenes* AR1193 was used for hairy root transformation experiments as described previously (Petit *et al.*, 1987; Stougaard *et al.*, 1987).

Tissue section and microscopy observation

For cross-sections of roots, shoots and nodules, tissue was fixed in a mixture of 4% (w/v) paraformaldehyde and 1% glutaraldehyde in 0.1 M phosphate buffer (pH 7.2). These samples were then embedded in Paraplast Plus (Sigma-Aldrich) by dehydrating with an ethanol and Lemosol[®] (Fujifilm Wako) series. Paraplast-blocks were sliced into semithin sections (12 μ m) using a PR-50 microtome (Yamato Kohki Industrial Co. Ltd, Saitama, Japan), and then stained with 0.5% toluidine blue. The sections were then observed under an Olympus BX53 microscope and phloem and xylem cells were counted by manual inspection. For expression analysis using *Pxy::GUS* and *Pxy::triple-YFP-nls*, transgenic hairy roots were

observed under an Olympus BX53 and a Zeiss Axioplan 2 microscope. For tissue sections, semithin sections of nodules and roots were prepared as previously described (Acosta-Jurado *et al.*, 2019). Semithin sections were stained in 0.5% toluidine blue and observed under an Olympus BX53 microscope.

Sequencing library preparation

Tissue was ground in liquid nitrogen to a very fine powder; 2 g of powder was transferred to 20 ml of ice-cold 1× HB buffer (0.1 M Tris, 0.8 M KCl, 0.1 M EDTA, 10 mM spermidine, 0.5 M sucrose, 0.5% Triton X-100, 0.15 β-mercaptoethanol, pH 9.4–9.5) in a 50 ml Falcon tube. After redissolving by gentle swirling on ice, the suspension was filtered through two layers of Miracloth, by squeezing with a gloved hand. Nuclei were then pelleted by centrifugation with a swinging bucket rotor at 1800 g for 15 min at 4°C. The pellet was resuspended in washing buffer (1× HB buffer without β-mercaptoethanol) and washed two or three times. Then the pellet was transferred into a new 1.5 ml Eppendorf tube and resuspended in 500 μl CTAB buffer (for 200 ml: 4 g CTAB, 16.36 NaCl, 10 ml 0.4 M EDTA pH 8.0, 20 ml 1 M Tris-HCl pH 8.0, H₂O to 200 ml) preheated to 60°C and incubated at 60°C for 30 min with regular mixing. Next, 500 μl chloroform : isoamyl alcohol (24 : 1) was added and contents were mixed by turning the tube until a uniform emulsion was formed. This step was followed by spinning at 5700 g, 4°C for 10 min and transferring the water phase to a new tube. Then, 5 μl RNase (10 mg ml⁻¹ stock) was added and the mixture was incubated at 37°C for 30 min and then put on ice for 5 min; 0.6 volumes of ice-cold isopropanol were added and the sample was incubated at -20°C overnight. To pellet the DNA, the sample was spun at 3200 g, 4°C for 6 min. Finally, the supernatant was discarded and the pellet was washed with 70% ethanol two times. After drying and resuspending in 55 μl water, the DNA concentration was measured on a NanoDrop 1000 spectrophotometer. The resulting DNA preparation was fragmented and sequenced by Fasteris (Switzerland) using the standard Illumina protocol for paired-end sequencing. The sequencing reads have been deposited at the Sequence Read Archive with accession number PRJNA623472 (<http://www.ncbi.nlm.nih.gov/bioproject/623472>).

Analysis of sequencing data

The sequencing reads from all pools were aligned to the MG20 reference genome v.2.5 and allele counts were extracted at all known polymorphic positions. Differences in allele frequencies were calculated using R, followed by sliding window analysis using a custom PERL script and plotting the results using R.

QTL analysis of *exoU* mutant nodulation of Gifu × MG20 recombinant inbred lines (RILs)

Gifu × MG20 RILs were scored for the average number of nodules formed with rhizobial *exoU* mutants and these observations, along with RIL genotypes, were used as input for QTL analysis.

Data were analysed using the mqm implementation in the R/QTL package v.1.21-2 (<http://www.rqtl.org/>). Following data import, data were converted to RIL format (convert2rself), missing genotypes were filled in (mqmaugment), and 1000 permutations were performed to determine significance thresholds (mqmpermutation).

Total RNA isolation and qRT-PCR

Total RNA from Gifu and MG20 roots inoculated with R7A or mock-inoculated was extracted using the NucleoSpin RNA plant extraction kit (Macherey-Nagel). Here, 2 μg total RNA from each sample was subjected to cDNA synthesis using M-MLV reverse transcriptase (Ambion). qRT-PCR was performed using the Thunderbird™ SYBR® qPCR mix (Toyobo) with the TaKaRa Thermal cycler Dice (TaKaRa Bio Inc., Shiga, Japan). Fold changes in expression were calculated using the $\Delta\Delta C_t$ method and normalised by *ATP synthase* expression. *ATP synthase* was amplified using primers (5'-CTTGAAGGAGAAC ATCACCAG-3' and 5'-CTGCCTTAGCAATCACCTCC-3'). For *Pxy*, primers (5'-AGTGGCAGATTTTGGGGTTG-3' and 5'-CGGATGAGTCCATGTCTG-3') were used.

Homology modelling

Models were generated using MODELLER (Webb & Sali, 2016) and HHPRED (Zimmermann *et al.*, 2018). A model of the Lotus PXY LRR domain was made using pdb 5JFK as a starting structural template. Tracheary element differentiation inhibitory factor (TDIF) peptide from the crystal structure of Arabidopsis PXY-TDIF (pdb 5GR9) (Zhang *et al.*, 2016) was superimposed onto the generated Lotus PXY LRR structure to visualise the putative peptide binding site. A model of the Lotus PXY kinase domain was made with pdb 2QKW as a starting structural template. The ATP analogue from pdb 5LPY was superimposed onto the generated Lotus PXY kinase structure to visualise the active site.

Results

Lotus japonicus ecotypes Gifu and MG20 show contrasting symbiotic phenotypes on inoculation with the *Mesorhizobium loti* *exoU* mutant

Previous studies have described a differential, quantitative symbiotic response to the *M. loti* *exoU* mutant among Lotus accessions, suggesting that the *exoU* response could be a multigene trait (Kelly *et al.*, 2013). To investigate this further, we focused on two accessions, Gifu and MG20 (Handberg & Stougaard, 1992; Kawaguchi *et al.*, 2001), which showed clearly contrasting phenotypes. When inoculated with the *exoU* deletion knockout mutant, Gifu formed small uninfected nodules (nodule primordia), while MG20 developed pink effective nodules (Fig. 1a,b). As the plants are grown under nitrogen-limited conditions, ineffective nodules result in nitrogen starvation and stunted growth. Here, c. 78% of the MG20 plants formed 1–6 pink, nitrogen-

fixing nodules per plant at 6 wk post inoculation, while Gifu plants did not form any pink nodules (Fig. 1c). Gifu and MG20 both showed significantly reduced infection thread numbers on inoculation with *exoU* as compared to inoculation with wild-type *M. loti* R7A (Fig. 1d).

QTL analysis using individual plants

As a first attempt to investigate the inheritance of the *exoU* response, we examined a Gifu × MG20 F2 population; *c.* 65% of the F2 plants formed nodules with an intermediate frequency, indicating that the trait was not monogenic (Fig. 1c). Genotyping the F2 plants that formed at least three pink nodules using SSR

markers (Hayashi *et al.*, 2001; Wang *et al.*, 2008), we identified two chromosomal regions associated with pink nodule formation, one at the end of chromosome 3 and one at the middle of chromosome 4 (Fig. 2a). These results suggested that the difference in *exoU* nodulation phenotype between Gifu and MG20 is genetically controlled and that the number of pink nodules is likely to be determined by multiple genes. As *Epr3* is on chromosome 2 at 23.28 Mbp, the single valine to isoleucine difference in the EPR3 amino acid sequences between Gifu and MG20 (BAI79284.1 and BAI79269.1) (Fig. S1) appears not to contribute, suggesting that variation in the response downstream of exopolysaccharide perception underlies the differential Gifu/MG20 *exoU* response.

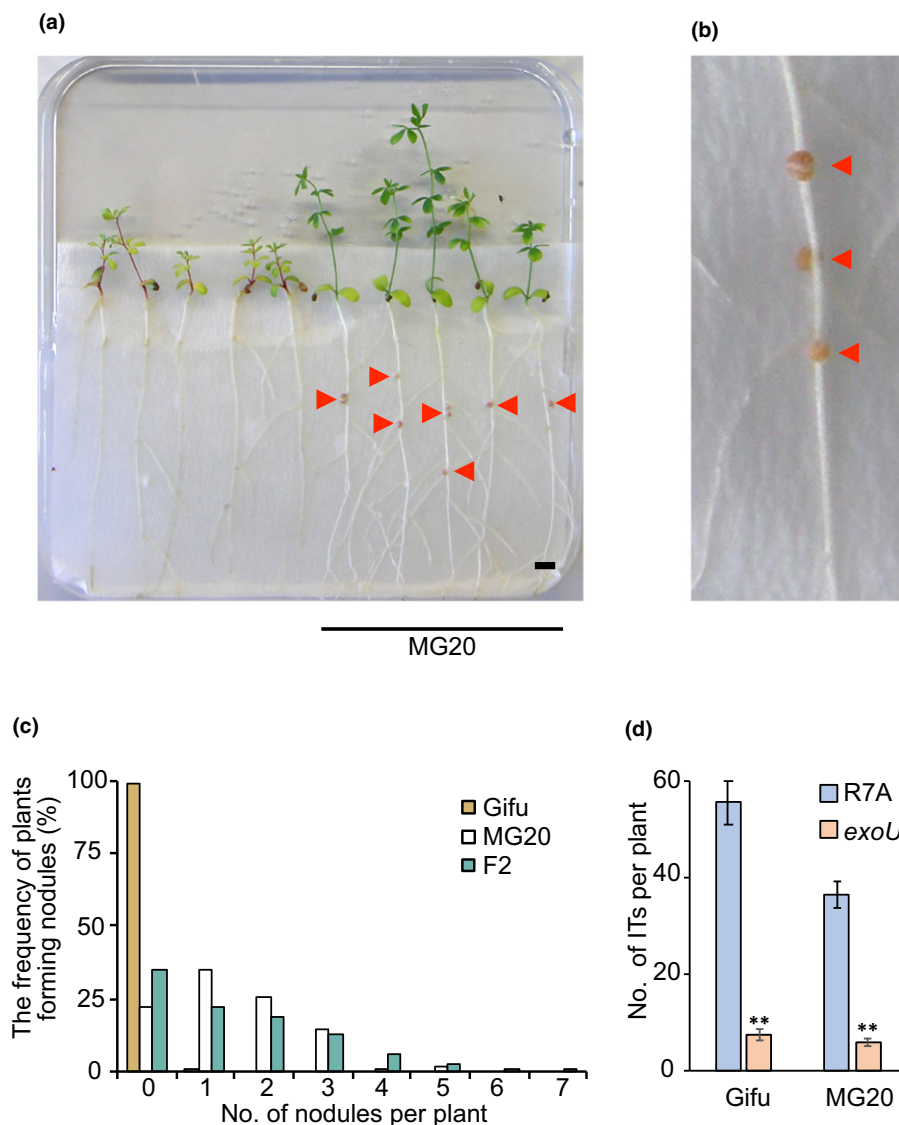


Fig. 1 *Mesorhizobium loti* *exoU* response in Lotus ecotypes Gifu, MG20 and F2 progeny. (a) Symbiotic phenotypes of Gifu and MG20 plants 6 wk post inoculation with the *M. loti* *exoU* mutant. (b) Infected pink nodules in MG20 inoculated with the *exoU* mutant. Red arrowheads show pink nodules in MG20 plants. Bar, 0.5 cm. (c) Frequency distribution of plants forming pink nodules in Gifu, MG20 and F2 progeny derived from the cross between Gifu and MG20 6 wk post inoculation with the *exoU* mutant. Numbers of phenotyped plants are: 98 (Gifu), 125 (MG20), and 319 (F2 progeny). (d) Infection thread formation in Gifu and MG20 10 d after inoculation with *M. loti* R7A or the *exoU* mutant. $n = 15$ in each experiment. **, $P < 0.01$, *t*-test, significant differences between R7A and *exoU* inoculation. Error bars, \pm SE.

To substantiate the F2 segregation analysis, we characterised the symbiotic phenotype of 114 RILs derived from a Gifu × MG20 cross (Hayashi *et al.*, 2001; Wang *et al.*, 2008), counting the number of *exoU*-induced nodules per plant (Table S3). The symbiotic phenotype and nodulation score were then analysed using R/QTL (Broman *et al.*, 2003), and we detected three chromosomal regions on chromosomes 2 and 3 associated with the number of pink nodules (Fig. 2b).

To further narrow down these regions we used RI-34, which has an MG20 genotype at the top of chromosome 2 and at the end of chromosome 3 and formed pink nodules with the *exoU* mutant (Fig. S2; Table S3). F2 plants from RI-34 back-crossed to Gifu were scored for symbiotic phenotype and genotyped. These F2 plants showed segregation for pink nodule formation, and a linkage analysis using SSR markers was therefore performed. Using plants forming at least three pink nodules, two genomic regions were detected (Fig. 2c). The region at the end of chromosome 3 was enriched for MG20 alleles, while the region at the centre of chromosome 5 showed enrichment of Gifu alleles (Fig. 2c). In all three linkage analyses, we consistently found enrichment of MG20 alleles at the end of chromosome 3 for plants forming *exoU* nodules, indicating that a major QTL was located there.

QTL-seq fine mapping of candidate genes on chromosome 3

To gain further genetic resolution, we took a QTL-seq approach and sequenced bulked segregant pools. To establish the bulks, a large MG20 × Gifu F2 population of 9766 plants inoculated with the *exoU* mutant was scored for the number of pink nodules and divided into two pools with contrasting phenotypes for collection of genomic DNA. Pool 1 consisted of 450 plants that formed at least three pink nodules and pool 2 comprised 6801 plants that did not develop any pink nodules. Another 2515 plants with intermediate phenotypes were discarded. Genomic DNA was extracted from pools 1 and 2 and sequenced on an Illumina Hi-Seq 2000 instrument, resulting in more than 100 million reads and 20× genome coverage per pool (Table S4).

We calculated allele frequencies for the two pools at all polymorphic positions and used this as a basis for sliding window analysis of allele frequency differences between the two pools. Sliding window size is a compromise between the signal stability achieved by averaging across many markers and the smoothing effect that may cause broadening of peaks or issues with detecting the correct position near the chromosome ends. We therefore tested a broad range of window sizes ranging from 250 to 1000 kb. Focusing on the bottom of chromosome 3, which was also robustly detected by the three mapping approaches based on genotyping and phenotyping of individual plants (Fig. 2a–c), we found a clear increase in allele frequency differences towards the end of the chromosome (Fig. 2d,e). The pool with at least three pink *exoU* nodules showed enrichment for MG20 alleles. This signal was detected regardless of the window size used (Fig. 2d,e) and was consistent with the RIL and F2 mapping results (Fig. 2a–c).

We then examined the results of the sliding window analyses in greater detail to accurately estimate the position of the allele frequency difference peak, at which the causal gene(s) should be located (Schneeberger *et al.*, 2009). Disregarding the plots with a 250 kb window size, which appeared too noisy, there was a clear trend in the allele frequency difference peak estimates: the larger the window size, the more the peak estimate shifted away from the chromosome end (Table S5). The reason for this trend was most likely the close proximity of the QTL to the end of the chromosome, where the last polymorphic SNP marker is found at 48.26 Mb, making it impossible for large sliding windows to detect peaks at the extreme end of the chromosome. As the peak estimates of the 500 and 750 kb windows were remarkably similar, we chose their average as the final peak position estimate of 47 712 169 bp (Table S5).

Pxy is a causal component of the differential *exoU* response

Sorting the candidate genes according to their peak distance identified *PHLOEM INTERCALATED WITH XYLEM* (*Pxy*, chr3.CM0261.600.r2.a in the Lotus MG20 genome assembly v2.5) and *XYLOGLUCAN ENDOGLUCOSYLASE/HYDROLASE 2* (*Xdh2*, chr3.CM0261.560.r2.a) as the closest nearby genes harbouring Gifu/MG20 polymorphisms (Table S6). Upon closer manual inspection of the region, an unannotated gene was also found. This was similar to *STRUCTURAL MAINTENANCE OF CHROMOSOMES* (*Smc6*) from Arabidopsis and harboured a large number of polymorphisms (Table S6). Resequencing of the candidate genes confirmed that they were intact in both ecotypes and verified Gifu/MG20 polymorphisms that resulted in amino acid substitutions (Fig. S3). To carry out complementation tests, these three genes or their coding sequences from Gifu and MG20 were fused to the Lotus ubiquitin promoter and transformed into Gifu or MG20 plants using *Agrobacterium rhizogenes* (Stougaard *et al.*, 1987; Stougaard, 1995; Maekawa *et al.*, 2008). The resulting transgenic hairy roots were inoculated with the *exoU* mutant and the symbiotic phenotype was scored. Regardless of the construct used, the transformed Gifu roots did not consistently form nodules, whereas the MG20 roots did form nodules (Tables 1,S7).

Considering the multigene inheritance suggested by the segregation analyses, Gifu × MG20 RILs RI-44, 56, 91, 94, 115, 120, 140 and 146 were then selected as recipients for candidate gene transformation (Tables 1,S7). These RILs showed a Gifu genotype between markers TM0091 and TM0127 in the chromosome 3 candidate region, and did not form pink nodules when inoculated with *exoU*. Among these RILs, only RI-94 transformed with *Pxy* from MG20 consistently formed nodules when inoculated with *exoU*, while the empty vector and *Xdh2* and *Smc6* from MG20, as well as *Pxy* from Gifu transformed into RI-94, resulted in formation of no or very few nodules (Tables 1,S7). Expression of MG20 *Pxy* resulted in a significant increase in the number of plants with nodules compared with the empty vector control and Gifu *Pxy* expression ($P < 0.0001$ and $P = 0.0113$ respectively, Fisher's exact test; Table 1). RI-94 nodulated normally with R7A (Table S8).

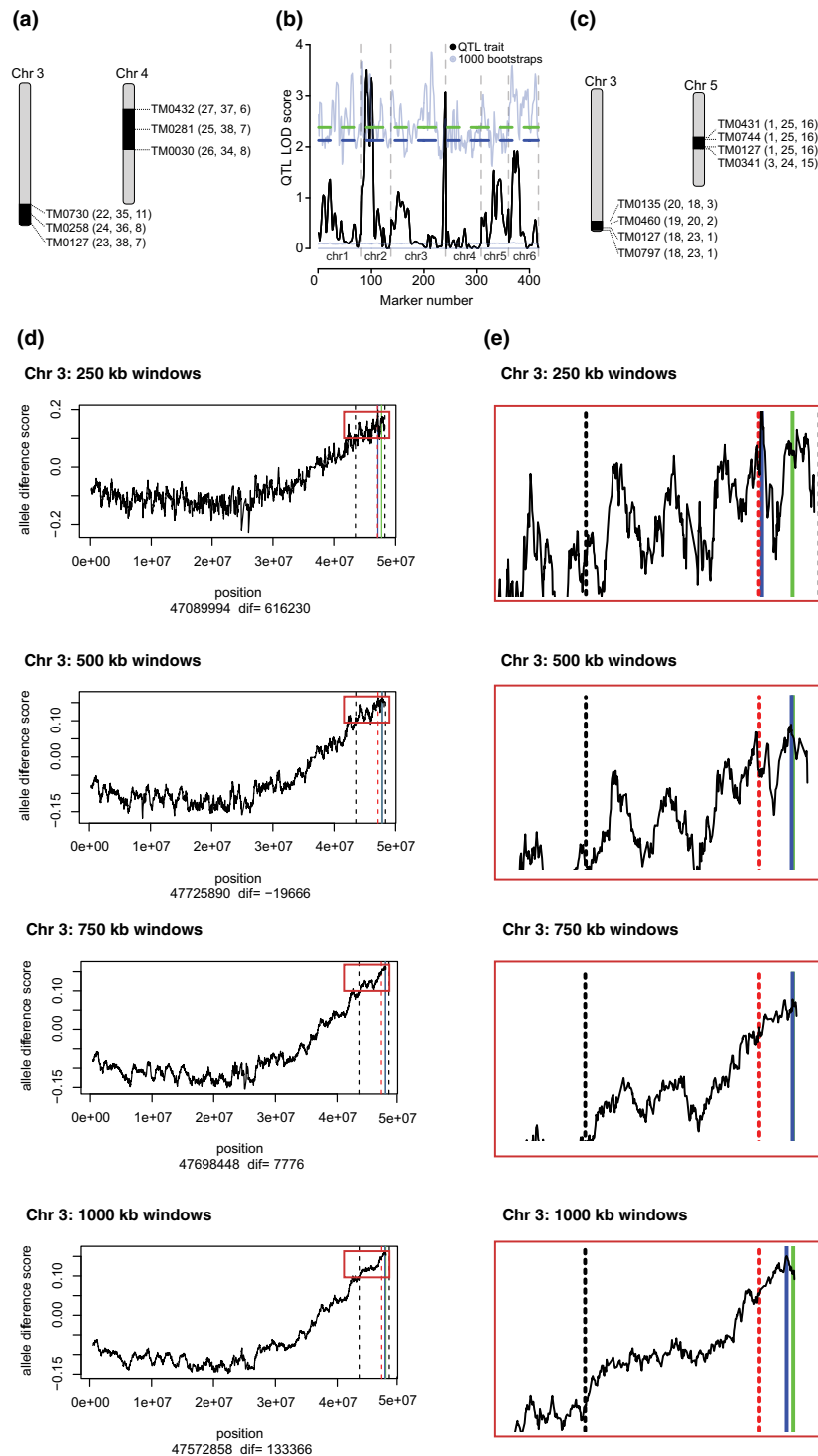


Fig. 2 QTL mapping of the *Lotus exoU* response. (a) Linkage analysis of symbiotic phenotypes in F₂ plants derived from the cross between Gifu and MG20. Plants forming more than three pink nodules after inoculation with the *exoU* mutant were selected and genotyped. (b) QTL analysis of *exoU* response based on analysis of Gifu × MG20 RILs. Quantitative trait scored was the average number of nodules after *exoU* inoculation; 5% and 10% false discovery rate levels are indicated by green and blue dashed lines, respectively. Light blue lines delimit the results of 1000 QTL analyses on permuted data, which were used to determine the significance thresholds. (c) Linkage analysis of symbiotic phenotypes in F₂ plants derived from the cross between Gifu and RI34, which is one of RILs forming pink nodules after *exoU* inoculation. Black areas identify candidate regions. (a, c) Numbers next to the SSR markers indicate numbers of individuals with MG20, heterozygous and Gifu genotypes, respectively. (d) Different sliding window sizes were used for QTL peak estimates on chromosome 3. Solid blue line indicates the peak estimate. Solid green line shows the position of the *Pxy* gene, whereas the red dashed lines indicate the genomic position of the closest linked marker according to the RIL-based QTL analysis. Leftmost dashed black line shows the position of the neighbouring flanking marker from the QTL analysis. The rightmost black line indicates the position of the last polymorphic SNP marker in the QTL-seq analysis. The exact position of the estimated peak and the distance (dif) between the peak estimate and the *Pxy* gene (blue and green lines) are indicated below the plot. (e) Close-ups of the regions marked by a red rectangle in the corresponding plots in panel (d).

Table 1 Lotus *Pxy* complementation experiment results.

Plant	Vector	Total no. of plants	No. of plants forming nodules	Total nodules	Pink nodule	White nodule	% (no. of plants forming nodules/total plants)
Gifu	pIV10	84	4	4	0	4	4.7
	pUbi:MG20 <i>Pxy</i>	90	5	6	0	6	5.6
	pUbi:Gifu <i>Pxy</i>	34	2	3	0	3	5.9
MG20	pIV10	114	23	29	10	19	20.2
	pUbi:MG20 <i>Pxy</i>	39	12	19	9	10	30.8
	pUbi:Gifu <i>Pxy</i>	39	8	14	8	6	20.5
RI94	pIV10	103	0	0	0	0	0
	pUbi:MG20 <i>Pxy</i>	110	22	26	10	16	20
	pUbi:Gifu <i>Pxy</i>	55	3	3	1	2	5.4

The *Pxy* gene encodes a leucine-rich repeat receptor-like kinase protein. The Lotus PXY amino acid sequence shares 65% identity and 78% similarity with Arabidopsis PXY, and Lotus PXY clusters with several plant PXY homologues, including Arabidopsis PXY in a phylogenetic tree of CLE peptide receptors (Fig. 3a; Table S9). In the 1976-bp putative *Pxy* promoter region, there are 12 SNPs and one single-base pair deletion between Gifu and MG20. We assayed *Pxy* expression levels in Gifu and MG20 compared with *ATP synthase* and found no significant differences (Fig. S4). The *Pxy* genes in Gifu and MG20 have three nonsynonymous SNPs in exonic regions and three SNPs and two deletions in intronic regions (Fig. 3b,c). One of the polymorphisms is found in the LRR5 region of Lotus PXY, where MG20 has an arginine in contrast to the Gifu glycine residue, which appears to be the more common variant across plant species (Fig. 3c). According to our homology model, this site is located close to the putative binding site of the TDIF peptide in the LRR domain⁵⁵ (Fig. 3d). Similarly, the I/R polymorphism is found near the ATP binding site in the PXY kinase domain (Fig. 3e).

The results of these complementation tests showed that the *Pxy* gene from MG20 allows development of pink nodules with the *exoU* mutant when transferred to a RIL containing the Gifu version of the gene, and that *Pxy* therefore is a causal component of the differential Gifu/MG20 response to *exoU* inoculation.

Pxy regulates nodule formation

To further investigate the role of PXY during symbiotic interactions, five *LORE1* mutant alleles (Urbański *et al.*, 2012; Małolepszy *et al.*, 2016), *pxy-1* to *pxy-5*, were obtained and characterised (Fig. 4a). On quarter-strength B&D medium without nitrate supplement, Gifu plants formed *c.* 5 pink nodules 5 wk post inoculation with *M. loti* R7A, while the *pxy-1* to *pxy-5* mutants developed two or three pink nodules (Fig. 4b,c). The structures of Gifu and *pxy* nodules were similar (Fig. 4b), but the shoot length in *pxy* mutants was about half that of the Gifu wild-type (Fig. 4d). In addition, the *pxy* mutants all showed significant reductions in lateral root formation (Fig. 4e). The five exonic *LORE1* alleles are all expected to represent gene knockouts (Małolepszy *et al.*, 2016), and this was consistent with the similar phenotypes observed across all alleles.

To further characterise the symbiotic phenotype, we repeated the nodulation experiment using modified Long Ashton medium (Fig. 4f–i). The *pxy* nodulation defects were more severe under these conditions, in which many white and nearly no pink nodules were formed (Fig. 4f,g).

To characterise *Rhizobium* infection in *pxy* mutants, we counted infection threads and observed nodule sections at 10 d or 14 d after inoculation with *M. loti* R7A. Gifu and *pxy* mutants showed similar numbers of infection threads and *Rhizobium* colonisation of nodule cells (Fig. 4h,i). These results suggested that PXY regulates nodule organ development but has little influence on the *Rhizobium* infection process.

Vascular differentiation in the *pxy* mutant

PXY functions in cambium proliferation and xylem differentiation (Etchells & Turner, 2010; Hirakawa *et al.*, 2010; Campbell *et al.*, 2016). In Arabidopsis, *pxy* mutants display a disorganised distribution of phloem and xylem in inflorescence stems and hypocotyls and a decrease in the number of xylem cells (Fisher & Turner, 2007; Hirakawa *et al.*, 2008). The vasculature of Arabidopsis *pxy* roots was reported to appear normal, but the number of lateral roots was reduced (Fisher & Turner, 2007; Etchells *et al.*, 2016). To examine vascular differentiation in Lotus *pxy* mutants, cross-sections were observed (Fig. 5). In the root cross-sections found at 1 cm from the root collar, the *pxy* root width was the same as that of Gifu, while the diameter of vascular bundles in *pxy* mutants was significantly smaller than that of Gifu (Fig. 5a–c). To measure the abundance of different cell types, the number of xylem and phloem cells was counted (Fig. 5d). No significant difference in phloem cell number between Gifu and *pxy* mutants was observed. However, the number of xylem cells was significantly decreased in the *pxy* mutants (Fig. 5a,b,d). Interestingly, secondary phloem cells next to the pericycle were properly distributed in Gifu but not in *pxy* mutants (Fig. 5a,b). This abnormal distribution of secondary phloem cells in the *pxy* mutant was also observed in the root at the base of nodules (Fig. 4i). In addition, *pxy* shoot cross-sections showed abnormal distribution of vascular bundles, and aberrant xylem and phloem differentiation (Fig. 5e). When plants were cultivated in the glasshouse supplemented with nitrate, *pxy* mutants grew normally for the first 6–7 wk, but then displayed growth

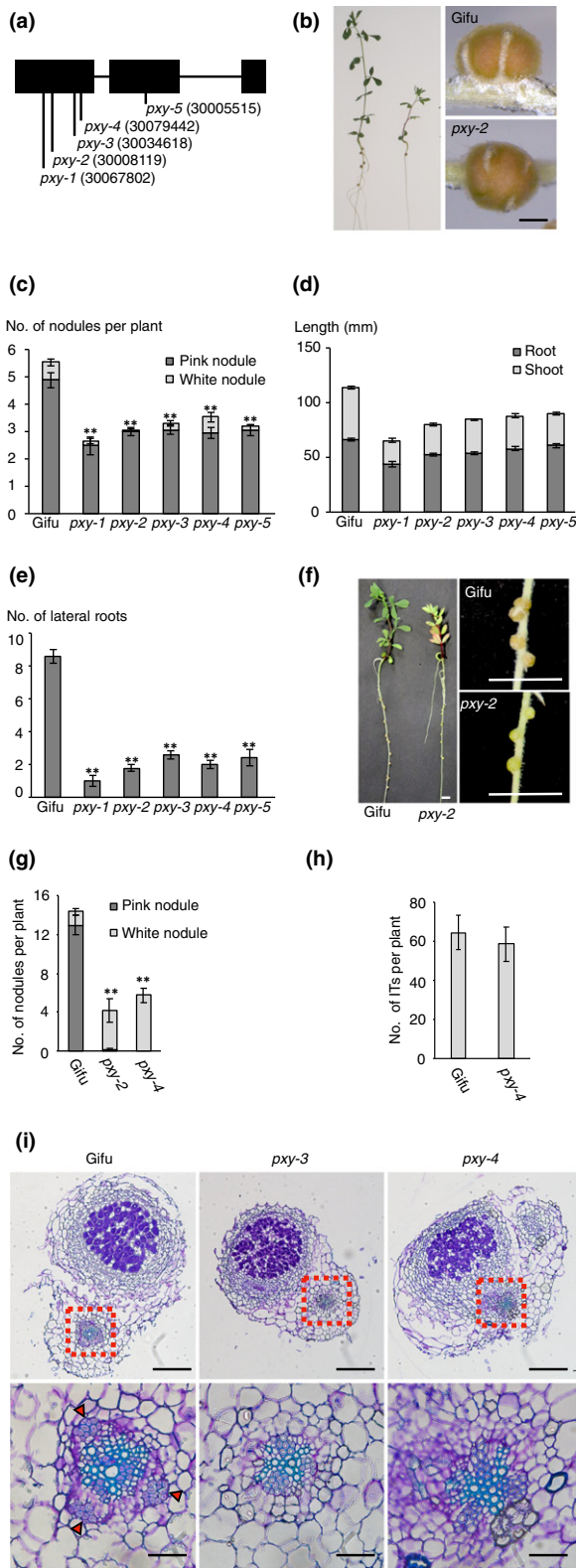


Fig. 4 Symbiotic phenotypes of Lotus Gifu *pxy* mutants. (a) Schematic gene model of Gifu *Pxy* showing the positions of *LORE1* retrotransposon insertions. Numbers in parenthesis are *LORE1* mutant line IDs as listed on Lotus Base (Mun *et al.*, 2016). (b–e) Symbiotic phenotypes of Gifu wild-type and *pxy* plants 5 wk post inoculation (wpi) with *Mesorhizobium loti* R7A wild-type on quarter-strength B&D medium. Bars, 1 cm (whole plants), 5 mm (nodules). (c) Average number of nodules per plant in Gifu and *pxy* mutants 5 wpi with *M. loti* R7A. (d) Average length of shoot and root in Gifu and *pxy* mutants 5 wpi with *M. loti* R7A. (e) Average number of lateral roots in Gifu and *pxy* mutants 5 wpi with *M. loti* R7A. (f, g) Symbiotic phenotype of *pxy* mutants 4 wk post inoculation (wpi) with *M. loti* R7A on Long Ashton medium. (f) Nodule structure of Gifu wild-type and *pxy* mutants 4 wpi with *M. loti* R7A. Bars, 0.5 cm. (g) Average number of nodules per plant in Gifu wild-type and *pxy* mutants 4 wpi with *M. loti* R7A. (h) Infection thread formation in Gifu and *pxy* 10 d after inoculation with *M. loti* R7A on Long Ashton medium. (i) Cross-sections of 2-wk-old white nodules in Gifu or *pxy* mutants inoculated with *M. loti* R7A. Upper panels are whole nodules and bottom panels are close-ups of the base of nodules in red dotted squares. Red arrowheads point to secondary phloem. Bars, 200 μ m (upper panels), 50 μ m (bottom panels). ******, $P < 0.01$, t -test, significant differences compared with Gifu plants. $n = 41$ (Gifu), 12 (*pxy-1*), 37 (*pxy-2*), 64 (*pxy-3*), 42 (*pxy-4*) and 24 (*pxy-5*) in (c–e), $n = 14$ (Gifu), 7 (*pxy-2*) and 7 (*pxy-4*) in g, $n = 6$ (Gifu) and 10 (*pxy-4*) in h. Error bars, \pm SE.

Pxy:triple-YFP-nls reporter gene expression in vascular bundles of the root meristems (Fig. 6). Similarly, *Pxy* expression was detected in cortical cells, where nodule and lateral root primordia emerged (Fig. 6), matching the phenotypic defects observed for these organs.

Discussion

In Lotus, perception of the wild-type octasaccharide or the *exoU* truncated pentasaccharide by EPR3 has a positive, respectively negative, effect in Gifu (Kawaharada *et al.*, 2015, 2017b) while the negative effect in MG20 is less pronounced. In this study, we carried out linkage analysis using F2 and RIL populations to understand the genetic basis of the differential *exoU* response in Lotus Gifu and MG20. We identified several genomic regions associated with the phenotype, indicating that the *exoU* response is a complex trait. *Epr3* (chr2.CM0008.630.r2.m, chr.2 position 23 273 436–23 278 205) is not located in any of the candidate intervals, making it unlikely that EPR3 *cis*-regulatory elements contribute to the intraspecific difference in the *exoU* response. Instead, we identified *Pxy* as the gene underlying a major QTL at the bottom of chromosome 3. Consistent with the involvement of multiple genes, MG20 *Pxy* did not rescue the Gifu phenotype in transformed roots. However, introduction of MG20 *Pxy* into RI-94 was sufficient to change the symbiotic phenotype and allow pink nodule formation with the *exoU* mutant. Interestingly, Gifu and MG20 showed the same pronounced reduction of *exoU* infection threads compared with wild-type R7A (Fig. 1d) and *pxy* mutants were not deficient in infection thread formation (Fig. 4h). By contrast, *pxy* nodule development was affected (Fig. 4f,g). Our results showed that MG20 *Pxy* acts together with other, as yet unknown, genes to allow nodule organogenesis and colonisation even when infection thread formation is strongly reduced.

arrest (Fig. S5). In addition, *pxy* mutants produced fewer lateral roots than Gifu (Figs 4e, S5).

These phenotypic observations showed that Lotus *PXY* has a function in regulation of both root and shoot vascular fate and phloem distribution. This finding is consistent with *Pxy:GFP* and

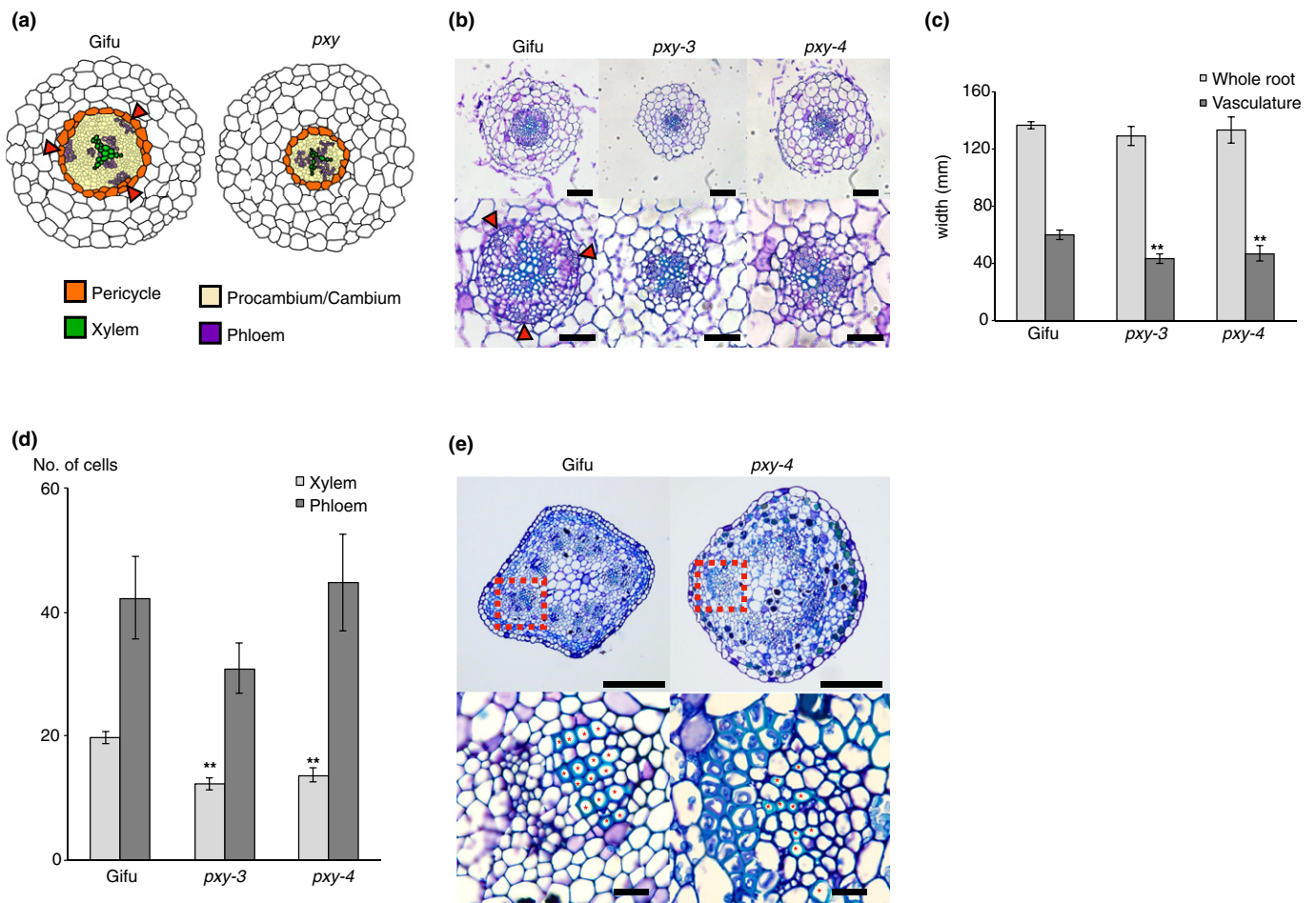


Fig. 5 Vascular organisation in *Lotus pxy* mutants. (a) Schematic cross-sections of Gifu and *pxy* roots. (b) Cross-sections Gifu, *pxy-3* and *pxy-4* 1-month-old roots. Upper panels show whole root sections, and lower panels show close-ups of the vasculature. Red arrowheads point to secondary phloem. Bars, 100 μ m (upper panels), 50 μ m (lower panels). (c) Average root width of Gifu and *pxy* mutants. (d) Average number of xylem and phloem cells in Gifu or *pxy* mutants. (c, d) Error bars, \pm SE. (e) Cross-sections of Gifu and *pxy-4* 2-month-old shoot. Upper panels are whole shoot sections and bottom panels are close-ups of the vascular bundles in the red dotted squares. Red stars indicate xylem cells. Bars, 200 μ m (upper panels), 50 μ m (lower panels). **, $P < 0.01$, t -test, significant differences compared with Gifu. $n = 6$ (Gifu), 8 (*pxy-3*) and 8 (*pxy-4*).

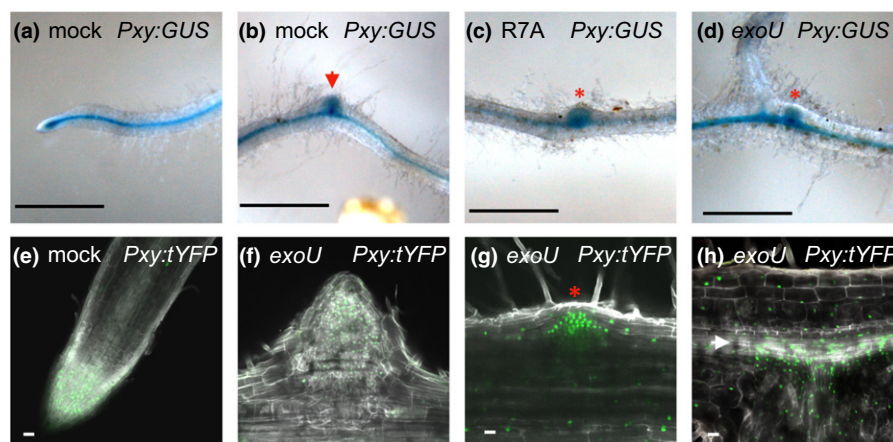


Fig. 6 *Lotus Pxy* expression in roots. Gifu transformed with a *Pxy:GUS* (a–d) or *Pxy:triple-YFP-nls* constructs (e–h). (a, b, e) Noninoculated. (c) 10 d post inoculation (dpi) with *Mesorhizobium loti* R7A. (d, f–h) 10 dpi with *exoU*. Red arrows, white arrow and red stars indicate lateral root primordia, vascular bundle and nodule primordia, respectively. Bars, 2 mm (a–d), 20 μ m (e–h).

Pxy was originally identified in *Arabidopsis* because its loss of function disrupted stem vascular structure, resulting in phloem intercalated with xylem (PXY), while the primary root vasculature remained unaffected (Fisher & Turner, 2007; Fukuda & Hardtke, 2020). This is in contrast to the *Lotus* root *pxy* phenotype described here, where the vasculature is clearly aberrant, in that the number of xylem cells is reduced and the secondary phloem cells are either absent or no longer distinct from the centrally located primary phloem cells (Figs 4,5). This finding suggests that the penetrance of PXY function is more pronounced in the complex tri-arch *Lotus* root than in the simpler diarch *Arabidopsis* root, which has very few files of phloem and xylem cells.

Shortly after its original discovery, PXY was rediscovered as the receptor for the CLE peptide TDIF and acquired the pseudonym TDR (TDIF receptor) (Hirakawa *et al.*, 2008). More recently, PXY has emerged as a hormonal signalling hub integrating CLE peptide, ethylene, auxin and cytokinin signalling. PXY suppresses ethylene signalling, and several ERF transcription factors showed increased expression in *Arabidopsis pxy* mutants (Etchells *et al.*, 2012). Ethylene, auxin and cytokinin are all involved in nodule organogenesis (Lin *et al.*, 2020), and hyperactivation of cytokinin can induce spontaneous nodule formation without rhizobia, which in turn facilitate infection (Tirichine *et al.*, 2007; Madsen *et al.*, 2010; Liu *et al.*, 2018a). Allelic differences in *Pxy*, and in other genes associated with the *exoU* QTL reported here, could therefore promote *exoU* nodulation through modulation of hormone signalling. In auxin and cytokinin signalling, respectively, PXY acts through two similar GSK (glycogen synthase kinase 3) proteins BIN2 (Brassinosteroid-insensitive 2, AT4G18710) and BIL1 (BIN2-like, AT1G06390) (Kondo *et al.*, 2014). The effects on vasculature phenotype of PXY modulation of cytokinin signalling through BIL1, MONOPTEROS and ARR7/15 were observed in *Arabidopsis* stems (Han *et al.*, 2018). By contrast, reduced formation of lateral roots was the phenotypic basis for the discovery of the PXY effects on auxin signalling through BIN2 and ARF7/19 (Cho *et al.*, 2014).

Mirroring the *Arabidopsis* phenotype, we observed a prominent decrease in lateral root formation in the *Lotus pxy* mutant (Figs 4e,S4), indicating a conserved role of PXY in lateral root formation. Interestingly, it has recently been shown that lateral roots and root nodules share a common developmental programme and that *ASL18/LBD16a* (*ASYMMETRIC LEAVES 2-LIKE 18/LATERAL ORGAN BOUNDARIES DOMAIN 16a*) is required for formation of both lateral root and nodule primordia in *Lotus* and *Medicago* (Schiessl *et al.*, 2019; Soyano *et al.*, 2019). In *Arabidopsis*, *ASL18/LBD16a* is under the control of Aux/IAA repressors and ARF7/19 (Okushima *et al.*, 2007; Goh *et al.*, 2012), which are in turn downstream of PXY/TDR. Based on our findings, PXY is an additional example of a regulator required for both lateral root and root nodule development that could act upstream of *ASL18/LBD16a*. This finding underlines the molecular genetic overlap between lateral root and root nodule organogenesis, although cellular origin and ontogeny of these lateral root organs is different.

In *Lotus*, three CLE peptides similar to TDIF are found on chromosomes 2, 4 and 6, and we identified *Lotus* homologues of

some genes that have been associated with PXY in *Arabidopsis* studies (Table S10). None of these were near the top of chromosome 2, where the only other significant signal, in addition to the *Pxy* QTL at the bottom of chromosome 3, was identified in our RIL-based QTL analysis (Fig. 2b). As there are no obvious candidate genes, more genetic fine mapping will be required to identify the remaining genes that caused the differential *exoU* response between Gifu and MG20.

We used the constitutive *Lotus* ubiquitin promoter to drive expression of the receptor-like kinase *Pxy*. Overexpression of the symbiotic receptor-like kinases *Nfr1*, *Nfr5* and *SymRK*, also from the ubiquitin promoter, resulted in spontaneous nodule formation (Ried *et al.*, 2014), demonstrating that the expression levels of receptor-like kinases can affect downstream signalling. We did not find major differences between Gifu and MG20 *Pxy* expression in roots (Fig. S4). In addition, the significant difference in nodulation resulting from overexpression of Gifu and MG20 *Pxy*, respectively, in the RI-94 background indicated that intraspecific differences cannot be explained only by differential expression and that important polymorphisms reside within the *Pxy* gene body (Table 1). This does not rule out a contribution from the *Pxy* promoter polymorphisms that could result in differences in PXY levels during specific stages of symbiotic interactions.

Three SNPs between Gifu and MG20 are located in the PXY coding region (Fig. 3). In an interspecific comparison, MG20 had an unusual glycine (G) to arginine (R) substitution (Fig. 3c). Similarly, *Lotus* intraspecific diversity data (Shah *et al.*, 2020) indicates that MG20 has unique alleles for the histidine/aspartate and isoleucine/arginine PXY polymorphisms in the population of re-sequenced Japanese accessions. *Pxy* could, therefore, not have been identified through GWAS using the current Japanese population sample, in which MG20 was collected from one of the southernmost locations (Shah *et al.*, 2020). It remains to be investigated how frequent is the MG20 *Pxy* genotype in other *Lotus* accessions originating near the MG20 collection site.

The G/R difference was found in the superhelical structure of the LRR5 motif in the extracellular domain (Fig. 3c,d). The glycine residue in Gifu was in a GxY motif that is conserved in other CLE peptide-type receptors in *Arabidopsis* and *Lotus* (Fig. 3c) (Morita *et al.*, 2016; Zhang *et al.*, 2016; Li *et al.*, 2017). Interestingly, the GxY motif in LRR5 of *Arabidopsis* PXY bound directly to the N-terminal of the TDIF peptide (Morita *et al.*, 2016; Zhang *et al.*, 2016; Li *et al.*, 2017) and the R/G polymorphism was near the residues directly responsible for binding (Fig. 3d). It is therefore conceivable that this Gifu/MG20 polymorphism may result in different TDIF binding affinities for Gifu and MG20 PXY receptors. This, in turn, could influence nodulation signalling and organogenesis, perhaps through effects on ethylene, auxin and cytokinin signalling, which are all implicated in both nodulation and PXY signalling (Bensmihen, 2015; Buhian & Bensmihen, 2018; Liu *et al.*, 2018b). Similarly, the I/R polymorphism (Fig. 3b) is located close to residues that bind ATP in the kinase domain (Fig. 3e) and may affect the level of kinase activity, thereby modulating downstream signalling. As both MG20 and Gifu retain normal vasculature and root growth,

PXY functionality is intact in both accessions and the substitutions would be expected to perturb, rather than disrupt, PXY peptide binding and kinase activity, which is consistent with the nature of the observed polymorphisms. Rather than directly affecting ligand binding or kinase activity, it is also possible that the polymorphisms could affect protein–protein interactions, or contribute to differences in PXY protein levels. Further work will be required to determine the precise effects of the individual polymorphisms.

Here, we have identified PXY as a causal component of a nodulation QTL. We have shown that the PXY effect on secondary growth is not limited to stem vasculature, as *Lotus pxy* roots showed clear aberrations in vascular structure. In addition, we found that PXY is required for normal formation of both lateral roots and root nodules. Our work is a striking example of how natural variation can result in a differential symbiotic response. It also provides novel insight into the function of a central regulator of the vascular organisation, tying PXY more firmly to root *de novo* organogenesis and highlighting the overlaps between genetic regulation of lateral root and nodule formation.


Acknowledgements


We wish to thank Yuki Kondo for discussion of PXY function and Sabine Zitzenbacher for technical assistance. This work was supported by the Danish Council for Independent Research | Technology and Production Sciences (10-081677) (SUA), Danish National Research Foundation (DNRF79) (JS), ERC advanced grant (268523) (JS), and Leading Initiative for Excellent Young Researchers (YK).

Author contributions


Symbiotic phenotyping, candidate gene testing, *pxy* mutant analysis, and expression analysis: YK, NS, HJ, MK, MZ, MT, HR. QTL-seq data analysis: VG, SUA, KS. PXY modelling analysis: KRA. Project planning and supervision: YK, KS, JS, SUA. Manuscript preparation: YK, SUA, JS.


ORCID


Kasper R. Andersen  <https://orcid.org/0000-0002-4415-8067>


Stig U. Andersen  <https://orcid.org/0000-0002-1096-1468>

Haojie Jin  <https://orcid.org/0000-0001-7460-4374>

Yasuyuki Kawaharada  <https://orcid.org/0000-0002-4756-4394>

Niels Sandal  <https://orcid.org/0000-0002-5230-2532>

Korbinian Schneeberger  <https://orcid.org/0000-0002-5512-0443>

Jens Stougaard  <https://orcid.org/0000-0002-9312-2685>

References

- Acosta-Jurado S, Rodríguez-Navarro DN, Kawaharada Y, Rodríguez-Carvajal MA, Gil-Serrano A, Soria-Díaz ME, Pérez-Montaño F, Fernández-Perea J, Niu Y, Alias-Villegas C *et al.* 2019. *Sinorhizobium fredii* HH103 *nolR* and *nodD2* mutants gain capacity for infection thread invasion of *Lotus japonicus* Gifu and *Lotus burttii*. *Environmental Microbiology* 21: 1718–1739.
- Ané JM, Kiss GB, Riely BK, Penmetsa RV, Oldroyd GED, Ayax C, Lévy J, Debelle F, Baek JM, Kalo P *et al.* 2004. *Medicago truncatula* DMI1 required for bacterial and fungal symbioses in legumes. *Science* 303: 1364–1367.
- Antolín-Llovera M, Ried MK, Parniske M. 2014. Cleavage of the symbiosis receptor-like kinase ectodomain promotes complex formation with nod factor receptor 5. *Current Biology* 24: 422–427.
- Arrighi JF, Godfroy O, De Billy F, Saurat O, Jauneau A, Gough C. 2008. The *RPG* gene of *Medicago truncatula* controls *Rhizobium*-directed polar growth during infection. *Proceedings of the National Academy of Sciences, USA* 105: 9817–9822.
- Bensmihen S. 2015. Hormonal control of lateral root and nodule development in legumes. *Plants* 4: 523–547.
- Broghammer A, Krusell L, Blaise M, Sauer J, Sullivan Jt, Maolanon N, Vinther M, Lorentzen A, Madsen Eb, Jensen Kj *et al.* 2012. Legume receptors perceive the rhizobial lipochitin oligosaccharide signal molecules by direct binding. *Proceedings of the National Academy of Sciences, USA* 109: 13859–13864.
- Broman KW, Wu H, Sen S, Churchill GA. 2003. R/qtl: QTL mapping in experimental crosses. *Bioinformatics* 19: 889–890.
- Buhian WP, Bensmihen S. 2018. Mini-review: nod factor regulation of phytohormone signaling and homeostasis during rhizobia-legume symbiosis. *Frontiers in Plant Science* 9: 1–8.
- Campbell L, Turner S, EtcHELLS P. 2016. Regulation of vascular cell division. *Journal of Experimental Botany* 68: 27–43.
- Cerri MR, Wang Q, Stolz P, Folgmann J, Frances L, Katzer K, Li X, Heckmann AB, Wang TL, Downie JA *et al.* 2017. The *ERN1* transcription factor gene is a target of the CcMK/CYCLOPS complex and controls rhizobial infection in *Lotus japonicus*. *New Phytologist* 215: 323–337.
- Charpentier M, Bredemeier R, Wanner G, Takeda N, Schleiff E, Parniske M. 2008. *Lotus japonicus* Castor and Pollux are ion channels essential for perinuclear calcium spiking in legume root endosymbiosis. *Plant Cell* 20: 3467–3479.
- Charpentier M, Sun J, Martins TV, Radhakrishnan GV, Findlay K, Soumpourou E, Thouin J, Véry A-A, Sanders D, Morris RJ, *et al.* 2016. Nuclear-localized cyclic nucleotide-gated channels mediate symbiotic calcium oscillations. *Science* 352: 1102–1105.
- Chiasson DM, Haage K, Sollweck K, Brachmann A, Dietrich P, Parniske M. 2017. A quantitative hypermorphic CNGC allele confers ectopic calcium flux and impairs cellular development. *eLife* 6: 1–15.
- Cho H, Ryu H, Rho S, Hill K, Smith S, Audenaert D, Park J, Han S, Beekman T, Bennett MJ *et al.* 2014. A secreted peptide acts on BIN2-mediated phosphorylation of ARFs to potentiate auxin response during lateral root development. *Nature Cell Biology* 16: 66–76.
- D'Haese W, Holsters M. 2002. Nod factor structures, responses, and perception during initiation of nodule development. *Glycobiology* 12: 79–105.
- EtcHELLS JP, Provost CM, Turner SR. 2012. Plant vascular cell division is maintained by an interaction between PXY and ethylene signalling. *PLoS Genetics* 8: e1002997.
- EtcHELLS JP, Smit ME, Gaudinier A, Williams CJ, Brady SM. 2016. A brief history of the TDIF-PXY signalling module: Balancing meristem identity and differentiation during vascular development. *New Phytologist* 209: 474–484.
- EtcHELLS JP, Turner SR. 2010. The PXY-CLE41 receptor ligand pair defines a multifunctional pathway that controls the rate and orientation of vascular cell division. *Development* 137: 767–774.
- Fisher K, Turner S. 2007. PXY, a receptor-like kinase essential for maintaining polarity during plant vascular-tissue development. *Current Biology* 17: 1061–1066.
- Fukuda H, Hardtke CS. 2020. Peptide signaling pathways in vascular differentiation. *Plant Physiology* 182: 1636–1644.
- Gleason C, Chaudhuri S, Yang T, Muñoz A, Poovaiah BW, Oldroyd GED. 2006. Nodulation independent of rhizobia induced by a calcium-activated kinase lacking autoinhibition. *Nature* 441: 1149–1152.
- Goh T, Joi S, Mimura T, Fukaki H. 2012. The establishment of asymmetry in *Arabidopsis* lateral root founder cells is regulated by LBD16/ASL18 and related LBD/ASL proteins. *Development* 139: 883–893.

- Groth M, Takeda N, Perry J, Uchid H, Dräxl S, Brachmann A, Sato S, Tabata S, Kawaguchi M, Wang TL *et al.* 2010. NENA, a *Lotus japonicus* homolog of Sec13, is required for rhizodermal infection by arbuscular mycorrhiza fungi and rhizobia but dispensable for cortical endosymbiotic development. *Plant Cell* 22: 2509–2526.
- Han S, Cho H, Noh J, Qi J, Jung H-J, Nam H, Lee S, Hwang D, Greb T, Hwang I. 2018. BIL1-mediated MP phosphorylation integrates PXY and cytokinin signalling in secondary growth. *Nature Plants* 4: 605–614.
- Handberg K, Stougaard J. 1992. *Lotus japonicus*, an autogamous, diploid legume species for classical and molecular genetics. *The Plant Journal* 2: 487–496.
- Hayashi M, Miyahara A, Sato S, Kato T, Yoshikawa M, Taketa M, Hayashi M, Pedrosa A, Onda R, Imaizumi-Anraku H *et al.* 2001. Construction of a genetic linkage map of the model legume *Lotus japonicus* using an intraspecific F2 population. *DNA Research* 8: 301–310.
- Heckmann AB, Lombardo F, Miwa H, Perry JA, Bunnewell S, Parniske M, Wang TL, Downie JA. 2006. *Lotus japonicus* nodulation requires two GRAS domain regulators, one of which is functionally conserved in a non-legume. *Plant Physiology* 142: 1739–1750.
- Hirakawa Y, Kondo Y, Fukuda H. 2010. Regulation of vascular development by CLE peptide-receptor systems. *Journal of Integrative Plant Biology* 52: 8–16.
- Hirakawa Y, Shinohara H, Kondo Y, Inoue A, Nakanomyo I, Ogawa M, Sawa S, Ohashi-Ito K, Matsubayashi Y, Fukuda H. 2008. Non-cell-autonomous control of vascular stem cell fate by a CLE peptide/receptor system. *Proceedings of the National Academy of Sciences, USA* 105: 15208–15213.
- Hirsch S, Kim J, Muñoz A, Heckmann AB, Downie JA, Oldroyd GED. 2009. GRAS proteins form a DNA binding complex to induce gene expression during nodulation signaling in *Medicago truncatula*. *Plant Cell* 21: 545–557.
- Hossain MS, Liao J, James EK, Sato S, Tabata S, Jurkiewicz A, Madsen LH, Stougaard J, Ross L, Szczygłowski K. 2012. *Lotus japonicus* ARPC1 is required for rhizobial infection. *Plant Physiology* 160: 917–928.
- Imaizumi-Anraku H, Takeda N, Charpentier M, Perry J, Miwa H, Umehara Y, Kouchi H, Murakami Y, Mulder L, Vickers K *et al.* 2005. Plastid proteins crucial for symbiotic fungal and bacterial entry into plant roots. *Nature* 433: 527–531.
- Kanamori N, Madsen LH, Radutoiu S, Frantescu M, Quistgaard EMH, Miwa H, Downie JA, James EK, Felle HH, Haaning LL *et al.* 2006. A nucleoporin is required for induction of Ca²⁺ spiking in legume nodule development and essential for rhizobial and fungal symbiosis. *Proceedings of the National Academy of Sciences, USA* 103: 359–364.
- Kawaguchi M, Motomura T, Imaizumi-Anraku H, Akao S, Kawasaki S. 2001. Providing the basis for genomics in *Lotus japonicus*: The accessions Miyakojima and Gifu are appropriate crossing partners for genetic analyses. *Molecular Genetics and Genomics* 266: 157–166.
- Kawaharada Y, James EK, Kelly S, Sandal N, Stougaard J. 2017a. The ethylene responsive factor required for nodulation 1 (ERN1) transcription factor is required for infection-thread formation in *Lotus japonicus*. *Molecular Plant-Microbe Interactions* 30: 194–204.
- Kawaharada Y, Kelly S, Nielsen MW, Hjuler Ct, Gysel K, Muszyński A, Carlson RW, Thygesen Mb, Sandal N, Asmussen Mh *et al.* 2015. Receptor-mediated exopolysaccharide perception controls bacterial infection. *Nature* 523: 308–312.
- Kawaharada Y, Nielsen MW, Kelly S, James EK, Andersen KR, Rasmussen SR, Füchtbauer W, Madsen LH, Heckmann AB, Radutoiu S *et al.* 2017b. Differential regulation of the *Epr3* receptor coordinates membrane-restricted rhizobial colonization of root nodule primordia. *Nature Communications* 8: 14534.
- Kelly SJ, Muszyński A, Kawaharada Y, Hubber AM, Sullivan JT, Sandal N, Carlson RW, Stougaard J, Ronson CW. 2013. Conditional requirement for exopolysaccharide in the *Mesorhizobium-Lotus* symbiosis. *Molecular Plant-Microbe Interactions* 26: 319–329.
- Kondo Y, Ito T, Nakagami H, Hirakawa Y, Saito M, Tamaki T, Shirasu K, Fukuda H. 2014. Plant GSK3 proteins regulate xylem cell differentiation downstream of TDIF–TDR signalling. *Nature Communications* 5: 3504.
- Lévy J, Bres C, Geurts R, Chalhou B, Kulikova O, Duc G, Journet E-P, Ané J-M, Lauber E, Bisseling T *et al.* 2004. A Putative Ca²⁺ and calmodulin-dependent protein kinase required. *Science* 303: 1361–1364.
- Li X, Zheng Z, Kong X, Xu J, Qiu L, Sun J, Reid D, Jin H, Andersen SU, Oldroyd GED *et al.* 2019. Atypical receptor kinase RINRK1 required for rhizobial infection but not nodule development in *Lotus japonicus*. *Plant physiology* 181: 804–816.
- Li Z, Chakraborty S, Xu G. 2017. Differential CLE peptide perception by plant receptors implicated from structural and functional analyses of TDIF-TDR interactions. *PLoS ONE* 12: 1–17.
- Lin J, Frank M, Reid D. 2020. No home without hormones: How plant hormones control legume nodule organogenesis. *Plant Communications* 1: 100104.
- Liu H, Sandal N, Andersen KR, James EK, Stougaard J, Kelly S, Kawaharada Y. 2018a. A genetic screen for plant mutants with altered nodulation phenotypes in response to rhizobial glycan mutants. *New Phytologist* 220: 526–538.
- Liu H, Zhang C, Yang J, Yu N, Wang E. 2018b. Hormone modulation of legume-rhizobial symbiosis. *Journal of Integrative Plant Biology* 60: 632–648.
- Madsen EB, Madsen LH, Radutoiu S, Olbryt M, Rakwalska M, Szczygłowski K, Sato S, Kaneko T, Tabata S, Sandal N *et al.* 2003. A receptor kinase gene of the LysM type is involved in legume perception of rhizobial signals. *Nature* 424: 637–640.
- Madsen LH, Tirichine L, Jurkiewicz A, Sullivan JT, Heckmann AB, Bek AS, Ronson CW, James EK, Stougaard J. 2010. The molecular network governing nodule organogenesis and infection in the model legume *Lotus japonicus*. *Nature Communications* 1: 10–12.
- Maekawa T, Kusakabe M, Shimoda Y, Sato S, Tabata S, Murooka Y, Hayashi M. 2008. Polyubiquitin promoter-based binary vectors for overexpression and gene silencing in *Lotus japonicus*. *Molecular Plant-Microbe Interactions* 21: 375–382.
- Maillet F, Fournier J, Mendis HC, Tadege M, Wen J, Ratet P, Mysore KS, Gough C, Jones KM. 2020. *Sinorhizobium meliloti* succinylated high-molecular-weight succinoglycan and the *Medicago truncatula* LysM receptor-like kinase MLYK10 participate independently in symbiotic infection. *The Plant Journal* 102: 311–326.
- Małolepszy A, Mun T, Sandal N, Gupta V, Dubin M, Urbański D, Shah N, Bachmann A, Fukai E, Hirakawa H *et al.* 2016. The *LORE1* insertion mutant resource. *The Plant Journal* 88: 306–317.
- Middleton PH, Jakob J, Penmetsa RV, Starkner CG, Doll J, Kaló P, Prabhu R, Marsh JF, Mitra RM, Kereszt A *et al.* 2007. An ERF transcription factor in *Medicago truncatula* that is essential for nod factor signal transduction. *Plant Cell* 19: 1221–1234.
- Mitra RM, Gleason CA, Edwards A, Hadfield J, Downie JA, Oldroyd GED, Long SR. 2004. A Ca²⁺/calmodulin-dependent protein kinase required for symbiotic nodule development: Gene identification by transcript-based cloning. *Proceedings of the National Academy of Sciences, USA* 101: 4701–4705.
- Morita J, Kato K, Nakane T, Kondo Y, Fukuda H, Nishimasu H, Ishitani R, Nureki O. 2016. Crystal structure of the plant receptor-like kinase TDR in complex with the TDIF peptide. *Nature Communications* 7: 12383.
- Mun T, Bachmann A, Gupta V, Stougaard J, Andersen SU. 2016. Lotus Base: An integrated information portal for the model legume *Lotus japonicus*. *Scientific Reports* 6: 1–18.
- Murakami E, Cheng J, Gysel K, Bozsoki Z, Kawaharada Y, Hjuler CT, Sørensen KK, Tao Ke, Kelly S, Venice F *et al.* 2018. Epidermal LysM receptor ensures robust symbiotic signalling in *Lotus japonicus*. *eLife* 7: 1–21.
- Murray JD, Muni RRD, Torres-Jerez I, Tang Y, Allen S, Andriankaja M, Li G, Laxmi A, Cheng X, Wen J *et al.* 2011. *Vapyrin*, a gene essential for intracellular progression of arbuscular mycorrhizal symbiosis, is also essential for infection by rhizobia in the nodule symbiosis of *Medicago truncatula*. *The Plant Journal* 65: 244–252.
- Nadzieja M, Kelly S, Stougaard J, Reid D. 2018. Epidermal auxin biosynthesis facilitates rhizobial infection in *Lotus japonicus*. *The Plant Journal* 95: 101–111.
- Nadzieja M, Stougaard J, Reid D. 2019. A toolkit for high resolution imaging of cell division and phytohormone signaling in legume roots and root nodules. *Frontiers in Plant Science* 10: 1–12.
- Nukui N, Ezura H, Yuhashi KI, Yasuta T, Minamisawa K. 2000. Effects of ethylene precursor and inhibitors for ethylene biosynthesis and perception on nodulation in *Lotus japonicus* and *Macroptilium atropurpureum*. *Plant and Cell Physiology* 41: 893–897.

- Okushima Y, Fukaki H, Onoda M, Theologis A, Tasaka M. 2007. ARF7 and ARF19 regulate lateral root formation via direct activation of LBD/ASL genes in Arabidopsis. *Plant Cell* 19: 118–130.
- Petit A, Stougaard J, Kühle A, Marcker KA, Tempé J. 1987. Transformation and regeneration of the legume *Lotus corniculatus*: A system for molecular studies of symbiotic nitrogen fixation. *Molecular and General Genetics* 207: 245–250.
- Qiu L, Lin JS, Xu J, Sato S, Parniske M, Wang TL, Downie JA, Xie F. 2015. SCARN a novel class of SCAR protein that is required for root-hair infection during legume nodulation. *PLoS Genetics* 11: 1–27.
- Radutoiu S, Madsen LH, Madsen EB, Felle HH, Umehara Y, Grønlund M, Sato S, Nakamura Y, Tabata S, Sandal N *et al.* 2003. Plant recognition of symbiotic bacteria requires two LysM receptor-like kinases. *Nature* 425: 585–592.
- Reid D, Liu H, Kelly S, Kawaharada Y, Mun T, Andersen SU, Desbrosses G, Stougaard J. 2018. Dynamics of ethylene production in response to compatible nod factor. *Plant Physiology* 176: 1764–1772.
- Reid D, Nadzieja M, Novák O, Heckmann AB, Sandal N, Stougaard J. 2017. Cytokinin biosynthesis promotes cortical cell responses during nodule development. *Plant Physiology* 175: 361–375.
- Ried MK, Antolín-Llovera M, Parniske M. 2014. Spontaneous symbiotic reprogramming of plant roots triggered by receptor-like kinases. *eLife* 3: 1–17.
- Saito K, Yoshikawa M, Yano K, Miwa H, Uchida H, Asamizu E, Sato S, Tabata S, Imaizumi-Anraku H, Umehara Y *et al.* 2007. Nucleoporin85 is required for calcium spiking, fungal and bacterial symbioses, and seed production in *Lotus japonicus*. *Plant Cell* 19: 610–624.
- Schauser L, Roussis A, Stiller J, Stougaard J. 1999. A plant regulator controlling development of symbiotic root nodules. *Nature* 402: 191–195.
- Schiessl K, Lilley JLS, Lee T, Tamvakis I, Kohlen W, Bailey PC, Thomas A, Luptak J, Ramakrishnan K, Carpenter MD *et al.* 2019. NODULE INCEPTION recruits the lateral root developmental program for symbiotic nodule organogenesis in *Medicago truncatula*. *Current Biology* 29: 3657–3668.e5.
- Schneeberger K, Ossowski S, Lanz C, Juul T, Petersen AH, Nielsen KL, Jørgensen J-E, Weigel D, Andersen SU. 2009. SHOREmap: simultaneous mapping and mutation identification by deep sequencing. *Nature Methods* 6: 550–551.
- Shah N, Wakabayashi T, Kawamura Y, Skovbjerg CK, Wang M-Z, Mustamin Y, Isomura Y, Gupta V, Jin H, Mun T *et al.* 2020. Extreme genetic signatures of local adaptation during *Lotus japonicus* colonization of Japan. *Nature Communications* 11: 1–15.
- Singh S, Parniske M. 2012. Activation of calcium- and calmodulin-dependent protein kinase (CCaMK), the central regulator of plant root endosymbiosis. *Current Opinion in Plant Biology* 15: 444–453.
- Sinharoy S, Liu C, Breakspear A, Guan D, Shailes S, Nakashima J, Zhang S, Wen J, Torres-Jerez I, Oldroyd G *et al.* 2016. A *Medicago truncatula* cystathionine- β -synthase-like domain-containing protein is required for rhizobial infection and symbiotic nitrogen fixation. *Plant Physiology* 170: 2204–2217.
- Soyano T, Shimoda Y, Kawaguchi M, Hayashi M. 2019. A shared gene drives lateral root development and root nodule symbiosis pathways in *Lotus*. *Science* 366: 1021–1023.
- Stougaard J. 1995. *Agrobacterium rhizogenes* as a vector for transforming higher plants. In: Jones H, ed. *Plant gene transfer and expression protocols. Methods in molecular biology*TM. Springer, 49–61.
- Stougaard J, Abildsten D, Marcker KA. 1987. The *Agrobacterium rhizogenes* pRI TL-DNA segment as a gene vector system for transformation of plants. *Molecular & General Genetics* 207: 251–255.
- Su C, Klein ML, Hernández-Reyes C, Batzenschlager M, Ditengou FA, Lacey B, Keller J, Delaux PM, Ott T. 2020. The *Medicago truncatula* DREPP protein triggers microtubule fragmentation in membrane nanodomains during symbiotic infections. *Plant Cell* 32: 1689–1702.
- Suzuki T, Takeda N, Nishida H, Hoshino M, Ito M, Misawa F, Handa Y, Miura K, Kawaguchi M. 2019. Lack of symbiont accommodation controls intracellular symbiont accommodation in root nodule and arbuscular mycorrhizal symbiosis in *Lotus japonicus*. *PLoS Genetics* 15: 1–25.
- Suzuki A, Suriyagoda L, Shigeyama T, Tominaga A, Sasaki M, Hiratsuka Y, Yoshinaga A, Arima S, Agarie S, Sakai T *et al.* 2011. *Lotus japonicus* nodulation is photomorphogenetically controlled by sensing the red/far red (R/FR) ratio through jasmonic acid (JA) signaling. *Proceedings of the National Academy of Sciences, USA* 108: 16837–16842.
- Tirichine L, Sandal N, Madsen LH, Radutoiu S, Albrektzen AS, Sato S, Asamizu E, Tabata S, Stougaard J. 2007. A gain-of-function mutation in a cytokinin receptor triggers spontaneous root nodule organogenesis. *Science* 315: 104–107.
- Tominaga A, Nagata M, Futsuki K, Abe H, Uchiumi T, Abe M, Kucho KI, Hashiguchi M, Akashi R, Hirsch AM *et al.* 2009. Enhanced nodulation and nitrogen fixation in the abscisic acid low-sensitive mutant enhanced nitrogen fixation1 of *Lotus japonicus*. *Plant Physiology* 151: 1965–1976.
- Urbański DF, Małolepszy A, Stougaard J, Andersen SU. 2012. Genome-wide LORE1 retrotransposon mutagenesis and high-throughput insertion detection in *Lotus japonicus*. *The Plant Journal* 69: 731–741.
- Wang X, Sato S, Tabata S, Kawasaki S. 2008. A High-density linkage map of *Lotus japonicus* based on AFLP and SSR markers. *DNA Research* 15: 323–332.
- Webb B, Sali A. 2016. Comparative protein structure modeling using MODELLER. *Current Protocols in Bioinformatics* 54: 1–5.
- Wong JEMM, Nadzieja M, Madsen LH, Bücherl CA, Dam S, Sandal NN, Couto D, Derbyshire P, Uldum-Berentsen M, Schroeder S *et al.* 2019. A *Lotus japonicus* cytoplasmic kinase connects Nod factor perception by the NFR5 LysM receptor to nodulation. *Proceedings of the National Academy of Sciences, USA* 116: 14339–14348.
- Xie F, Murray JD, Kim J, Heckmann AB, Edwards A, Oldroyd GED, Downie JA. 2012. Legume pectate lyase required for root infection by rhizobia. *Proceedings of the National Academy of Sciences, USA* 109: 633–638.
- Yano K, Aoki S, Liu M, Umehara Y, Suganuma N, Iwasaki W, Sato S, Soyano T, Kouchi H, Kawaguchi M. 2017. Function and evolution of a *Lotus japonicus* AP2/ERF family transcription factor that is required for development of infection threads. *DNA Research* 24: 193–203.
- Yano K, Shibata S, Chen W-L, Sato S, Kaneko T, Jurkiewicz A, Sandal N, Banba M, Imaizumi-Anraku H, Kojima T *et al.* 2009. CERBERUS, a novel U-box protein containing WD-40 repeats, is required for formation of the infection thread and nodule development in the legume-Rhizobium symbiosis. *The Plant Journal* 60: 168–180.
- Yokota K, Fukai E, Madsen LH, Jurkiewicz A, Rueda P, Radutoiu S, Held M, Hossain MS, Szczygłowski K, Morieri G *et al.* 2009. Rearrangement of actin cytoskeleton mediates invasion of *Lotus japonicus* roots by *Mesorhizobium loti*. *Plant Cell* 21: 267–284.
- Zhang H, Lin X, Han Z, Qu LJ, Chai J. 2016. Crystal structure of PXY-TDIF complex reveals a conserved recognition mechanism among CLE peptide-receptor pairs. *Cell Research* 26: 543–555.
- Zimmermann L, Stephens A, Nam SZ, Rau D, Kübler J, Lozajic M, Gabler F, Söding J, Lupas AN, Alva V. 2018. A completely reimplemented MPI bioinformatics Toolkit with a new HHpred server at its Core. *Journal of Molecular Biology* 430: 2237–2243.

Supporting Information

Additional Supporting Information may be found online in the Supporting Information section at the end of the article.

Fig. S1 Alignment of EPR3 receptor protein sequences from MG20 and Gifu.

Fig. S2 Illustration of *Lotus* MG20 \times Gifu RIL genotypes.

Fig. S3 *Xdh2* and *Smc6* polymorphisms.

Fig. S4 *Lotus Pxy* expression.

Fig. S5 *pxy* mutant phenotypes.

Table S1 Recipes for quarter-strength B&D and modified Long Ashton medium.

Table S2 Primers for genotyping of *Pxy* *LORE1* mutants.

Table S3 Average number of *exoU* nodules in recombinant inbred lines.

Table S4 Deep sequencing read depths.

Table S5 Peak estimates for the *exoU* nodulation QTL on chromosome 3.

Table S6 Gifu/MG20 polymorphisms for genes located at the end of chromosome 3.

Table S7 Gifu, MG20 and Gifu × M20 RIL complementation experiment results.

Table S8 RI-94 nodulation with *M. loti* R7A.

Table S9 Accession numbers for CLE peptide receptors.

Table S10 Lotus homologues of PXY-associated genes.

Please note: Wiley Blackwell are not responsible for the content or functionality of any Supporting Information supplied by the authors. Any queries (other than missing material) should be directed to the *New Phytologist* Central Office.



About *New Phytologist*

- *New Phytologist* is an electronic (online-only) journal owned by the New Phytologist Foundation, a **not-for-profit organization** dedicated to the promotion of plant science, facilitating projects from symposia to free access for our Tansley reviews and Tansley insights.
- Regular papers, Letters, Viewpoints, Research reviews, Rapid reports and both Modelling/Theory and Methods papers are encouraged. We are committed to rapid processing, from online submission through to publication 'as ready' via *Early View* – our average time to decision is <26 days. There are **no page or colour charges** and a PDF version will be provided for each article.
- The journal is available online at Wiley Online Library. Visit **www.newphytologist.com** to search the articles and register for table of contents email alerts.
- If you have any questions, do get in touch with Central Office (np-centraloffice@lancaster.ac.uk) or, if it is more convenient, our USA Office (np-usaoffice@lancaster.ac.uk)
- For submission instructions, subscription and all the latest information visit **www.newphytologist.com**